Chapter 2

Observational Constraints on Exotic Matter in Emergent Universe

2.1 Introduction

EU model proposed by Mukherjee *et al.* [68] in GTR is considered to be an important cosmological model of the universe which is ever existing having no initial singularity and which accommodates a late accelerating phase satisfactorily. In EU model, the universe began to expand from an initial non-singular phase, thereafter smoothly joins with a phase of exponential inflation followed by a standard reheating phase and finally it approaches the classical thermal radiation dominated era analogous to the conventional Big Bang model [69].

The EoS for EU model contains two parameters A and B where $A > 0$. The peculiarity of the model obtained by Mukherjee *et al.* [68] is that it permits a universe with a composition of three types of fluid determined by one parameter B (shown in Table-(1.1)).

It may be mentioned here that in EoS eq. (1.3) for $\alpha = -\frac{1}{2}$, it leads to the EoS required for emergent universe (EU) model. Subsequently existence of EU model in Gauss-Bonnet gravity [86], Brane world gravity [67, 84], Brans-Dicke theory [98] have been examined. Universe in this model is sufficiently big enough to begin with which might stay at the phase for a large enough time to avoid quantum gravitational effects even in the very early universe. Therefore the quantum gravity effect can be avoided. The EoS parameters A, B are arbitrary which can be determined from the observational data. Initially the best-fitted EoS parameters A, B with integration constant K are determined using the observed data set. It is thus worth to investigate the viability of such an EU model with the recent observational data. Nevertheless we intend to explore in this Chapter the allowed range of values of the parameter A ($A > 0$), B for a viable cosmological scenario by observations.

To determine the range of values for A and B permitted by observations we adopt the following techniques as follows: (i) χ^2 minimization technique corresponding to $H(z)$ *vs.* z data (OHD) [99] given in Table-(2.1), (ii) joint analysis of $H(z)$ *vs.* z data and a model independent BAO peak parameter and (iii) joint analysis of $H(z)$ *vs.* z data, BAO peak parameter and CMB shift parameter together. We explore here the suitability of the model with the help of supernovae data (union compilation data) finally.

Table 2.1: $H(z)$ *vs.* z data (OHD) [99]

z *Data*	$H(z)$	σ
0.00	73	± 8.0
0.10	69	$\pm$ 12.0
0.17	83	± 8.0
0.27	77	$\pm$ 14.0
0.40	95	$\pm$ 17.4
0.48	90	$\pm$ 60.0
0.88	97	$\pm$ 40.4
0.90	117	$\pm$ 23.0
1.30	168	$\pm$ 17.4
1.43	177	$\pm$ 18.2
1.53	140	$\pm$ 14.0
1.75	202	$\pm$ 40.4

2.2 Field equations

The Hubble parameter (H) in terms of redshift parameter z is written as

$$H(z) = -\frac{1}{1+z}\frac{dz}{dt} \tag{2.1}$$

using $a = \frac{1}{1+z}$, taking a_0(a at the present time)= 1. Since components of matter (baryon) and dark energy (exotic matter) are conserved separately, we use energy conservation equation together with EoS given by eq. (1.18) to determine the expression for the energy density. Consequently eq. (1.12) yields:

$$\rho_{emu} = \left[\frac{A}{1+B} + \frac{1}{B+1}\frac{K}{a^{\frac{3(B+1)}{2}}}\right]^2, \tag{2.2}$$

where K is an integration constant which is positive quantity. From eq. (2.2) it is evident that the energy density is composed of three different terms, where a constant term $(\frac{A}{1+B})^2$ may be identified with a cosmological constant and the other two terms are identified with two different types of fluid determined by the parameter B. Using the Friedmann equation (1.9) we express H in terms of redshift parameter z for the

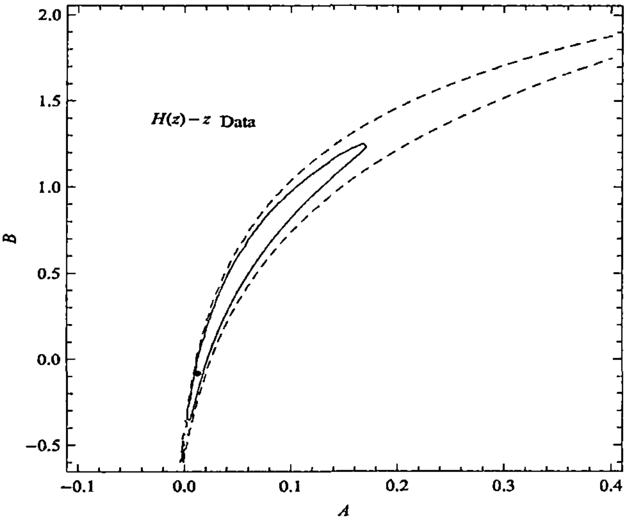

Figure 2.1: $A - B$ contours using $H(z)$ *vs.* z data (OHD) for $K = 0.0100$ at 95.4% (Solid) and 99.7% (Dashed) confidence level. The best-fit point is shown (0.0122, −0.0823).

model, which is given by

$$H(z) = H_0 \left[\Omega_{b_0}(1+z)^3 + (1-\Omega_{b_0}) \left(\frac{A + K(1+z)^{\frac{3(B+1)}{2}}}{A+K} \right)^2 \right]^{\frac{1}{2}}, \tag{2.3}$$

with $\Omega = \Omega_{b_0} + \Omega_{em_0} = 1$, where Ω is composed of baryon and exotic fluids. Ω_{b_0} represents baryon energy density and Ω_{em_0} represents the exotic fluid density.

2.3 $(H(z) - z)$ data (OHD) as a constraining tool

The EU model obtained by Mukherjee *et al.* [68] is implemented in a flat universe. Consequently we consider a composition of baryonic matter and the exotic matter in a flat Friedmann universe permitted by EoS given by eq. (1.18) to constrain the EoS parameters. The Hubble parameter given by eq. (2.3) is a function of a number of variables, which can be re-written as :

$$H^2(H_0, A, B, K, z) = H_0^2 E^2(A, B, K, z), \tag{2.4}$$

where

$$E(A, B, K, z) = \left[\Omega_{b_0}(1+z)^3 + (1-\Omega_{b_0})\left(\frac{A + K(1+z)^{\frac{3(B+1)}{2}}}{A+K}\right)^2\right]^{\frac{1}{2}} \tag{2.5}$$

is the dimensionless Hubble parameter. The best-fit values for the unknown parameters of the model, namely A, B and K are determined by minimizing $\chi^2_{(H-z)}$ function which is given below

$$\chi^2_{(H-z)}(H_0, A, B, K, z) = \sum \frac{[H(H_0, A, B, K, z) - H_{obs}(z)]^2}{\sigma_z^2} \tag{2.6}$$

where $H_{obs}(z)$ is the observed Hubble parameter at redshift z and σ_z is the error associated with that particular observation, the suffix $(H - z)$ corresponds to use of Hubble parameter *vs.* redshift data [99]. Since we are interested in determining the model parameters, H_0 is not important for our analysis. So we marginalize the function over H_0 to get the probability distribution function in terms of A, B, K only, which is given by

$$L(A, B, K) = \int dH_0 P(H_0) \exp\left(\frac{-\chi^2_{(H-z)}(H_0, A, B, K, z)}{2}\right), \tag{2.7}$$

where $P(H_0)$ is the prior distribution function for the present Hubble constant. Here we consider Gaussian priors with $H_0 = 72 \pm 8$ [100]. The function χ^2 is minimized by maximizing the likelihood function $L(A, B, K)$. We fix K at the best-fitted value and contours in A-B plane are drawn at different confidence limit. However, fixing of K is allowed as we are interested to obtain range of A and B which is related to the EoS

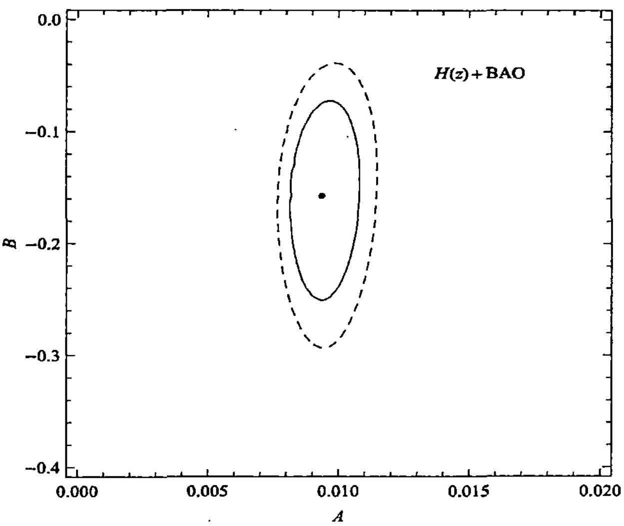

Figure 2.2: $A - B$ contours using OHD data and BAO peak parameter with $K = 0.0101$. 95.4% (Solid) and 99.7% (Dashed) confidence levels are shown in the figure along with the best-fit value (0.0094, -0.1573)

given by eq. (1.18). K enters in the theory as an integration constant which is always positive ($K > 0$). In fig. (2.1) we draw 95.4% and 99.7% contours on A-B plane. We see that within 95.4% confidence limit A and B lies in the range $-0.0011 \leq A \leq 0.1731$ and $-0.5864 \leq B \leq 1.254$. We see that within 99.7% confidence limit A and B lies in the range $-0.0022 \leq A \leq 0.389$ and $-0.5949 \leq B \leq 1.663$. A positive value of A permits a viable cosmological scenario.

2.4 Joint analysis with *OHD* and BAO peak parameter

In this section we use the technique adopted by [88] to study the BAO peak parameter $\mathcal{A}$ (which is determined by A). For a flat universe $\mathcal{A}$ is given by eq. (1.30) with $\Omega_m = \Omega_b + (1 - \Omega_b)(1 - \frac{A}{K+A})^2$. From observations, we get the values

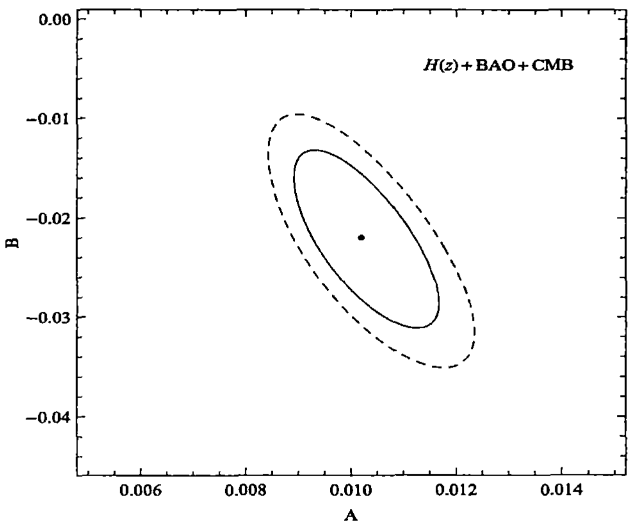

Figure 2.3: $A - B$ contours using OHD data, BAO peak parameter and CMB shift parameter for $K = 0.0102$. 95.4% (Solid) and 99.7% (Dashed) confidence levels are shown in the figure along with the best-fit value (0.0103, -0.0219)

$\mathcal{A} = 0.469 \pm 0.017$ at $z_1 = 0.35$. For joint analysis we consider $\chi^2_{joint} = \chi^2_{(H-z)} + \chi^2_{BAO}$ where χ^2_{BAO} is given by eq. (1.31). The joint analysis with BAO here sets a new constraints on A and B, which are $0.0082 \leq A \leq 0.0108$ and $-0.2527 \leq B \leq -0.0715$ up to 95.4% confidence level and $0.0077 \leq A \leq 0.0116$ and $-0.3053 \leq B \leq -0.0306$ up to 99.7% confidence level.

2.5 Joint analysis with OHD, BAO peak parameter and CMB shift parameter ($\mathcal{R}$)

In this section we use CMB shift parameter ($\mathcal{R}$) given by eq. (1.34). The WMAP 3 data gives us $\mathcal{R} = 1.70 \pm 0.03$ [101]. Thus we define $\chi^2_{CMB} = \frac{(\mathcal{R}-1.70)^2}{(0.03)^2}$ in $\chi^2_{Tot} = \chi^2_{(H-z)} + \chi^2_{BAO} + \chi^2_{CMB}$ which impose additional constraints on the model parameters. The statistical analysis with χ^2_{Tot} further tightens up the bounds on A and B. In fig.

Data	A	B	K
OHD	0.0122	-0.0823	0.0100
$OHD + BAO$	0.0094	-0.1573	0.0101
$OHD + BAO + CMB$	0.0103	-0.0219	0.0102

Table 2.2: Best-fit values of the EoS parameters

Data	CL	A	B
OHD	95.4%	$(-0.0011,\ 0.1731)$	$(-0.5864,\ 1.254)$
	99.7%	$(-0.0022,\ 0.389)$	$(-0.5949,\ 1.663)$
$OHD + BAO$	95.4%	$(0.0082,\ 0.0108)$	$(-0.2527, -0.0715)$
	99.7%	$(0.0077,\ 0.0116)$	$(-0.3053, -0.0306)$
$OHD + BAO + CMB$	95.4%	$(0.0089,\ 0.0117)$	$(-0.0313, -0.0131)$
	99.7%	$(0.0080,\ 0.013)$	$(-0.037,\ -0.009)$

Table 2.3: Range of values of the EoS parameters using OHD+BAO+CMB data

(2.3), 95.4% and 99.7% contours are plotted on A-B plane. We determine constraints from this analysis: within 95.4% confidence limit we get $0.0089 \leq A \leq 0.0117$ and $-0.0313 \leq B \leq -0.0131$. However, within 99.7% confidence level $0.008 \leq A \leq 0.013$ and $-0.037 \leq B \leq -0.009$. The best-fit value obtained here is given by $A = 0.0103$, $B = -0.0219$ and $K = 0.0102$. The best-fit values of the model parameters obtained from different data are shown in Table-(2.2) and the corresponding range are shown in Table-(2.3). Finally we draw a supernovae magnitudes $\mu(z)$ *vs.* redshift z curve for our model with the best-fit values of A, B and K and also show the same curve drawn from union compilation data for SNeIa [102] in fig. (2.4).

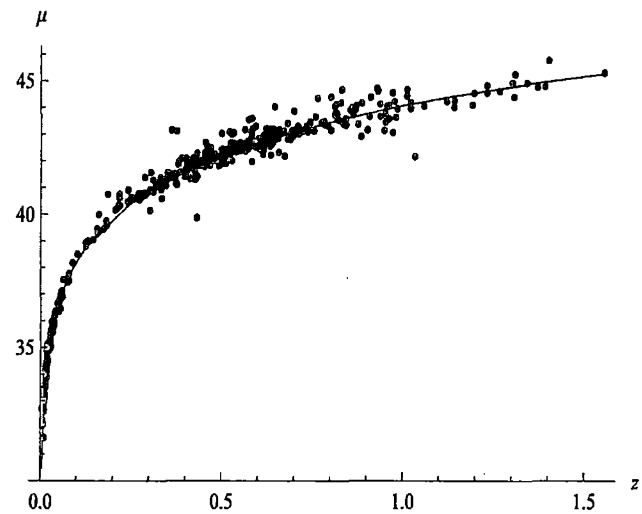

Figure 2.4: Comparison of $\mu(z)$ *vs.* z curve with supernovae data

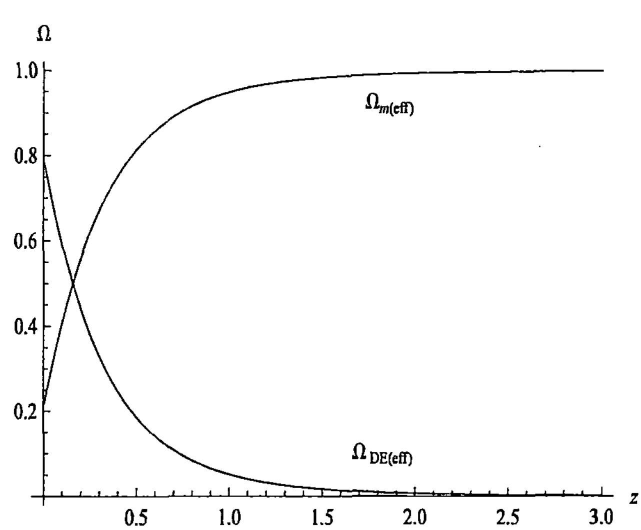

Figure 2.5: Variation of density parameter (Ω) for effective dark energy and effective matter content of the universe with redshift.

2.6 Discussions

The emergent universe model obtained with a non-linear equation of state contains two arbitrary parameters A and B which are determined using observational data. We obtain range of values of the EoS parameters by numerical analysis. The best-fit values of A and B are determined which are given by $A = 0.0103$, $B = -0.0219$ with integration constant $K = 0.0102$. Within 99.7% confidence level the parameter A and B lies in the following range $0.008 \leq A \leq 0.013$ and $-0.037 \leq B \leq -0.009$. The evolution of various cosmological parameters of the model are also studied. The density parameter for effective dark energy and effective matter content of the universe with the redshift are plotted in fig. (2.5). It is noted that almost 80% of the present matter-energy content is dominated by effective dark energy and the remaining constituents are baryonic and non-baryonic matters. The effective equation of state (ω_{eff}) for EU remains negative which is plotted in fig. (2.6 a). The transition of the universe from a deceleration phase to an accelerating phase in recent past is evident from the plot of deceleration parameter against redshift in fig. (2.6 b). Supernovae magnitudes $\mu(z)$ *vs.* redshift z curve is drawn at the best-fit values of A, B and K and compared with union compilation data for SNeIa [102] in fig. (2.4). The results are in agreement with observations.

[1]

[1]* We use EoS for emergent universe $p = B\rho - A\rho^{\frac{1}{2}}$ which is different from that used in the published paper $p = A\rho - B\rho^{\frac{1}{2}}$ for a consistent representation with MCG

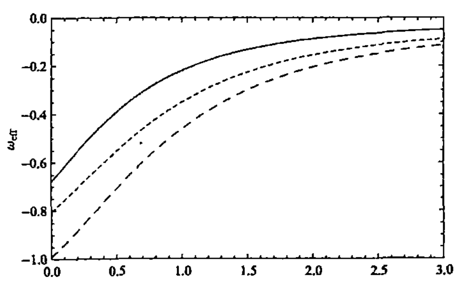

(a)

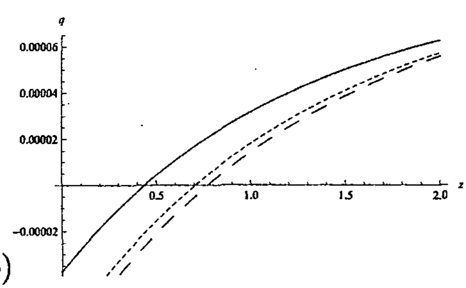

(b)

Figure 2.6: (a) Variation of effective EoS parameter for EU (ω_{eff}) with redshift (z). (b) Variation of deceleration parameter (q) with redshift (z). Solid, Dashed and Dotted line corresponds to the best-fit values, 95.4% confidence level and 99.7% confidence level respectively.